Nonlinear betatron dynamics near the linear and nonlinear difference resonances

S. Kladov and E. Perevedentsev
Budker Institute of Nuclear Physics, Novosibirsk, 630090 Russia
also at Novosibirsk State University, Novosibirsk, 630090 Russia

Abstract

In the vicinity of the linear coupling resonance where the operating point of the collider is positioned, we study the effect of nonlinear coupling resonances on the single-particle phase space, beam sizes and the waveform of coherent beam motion. The latter is interesting for diagnostics of the nonlinear dynamics.

In this paper non-linear particle dynamics effects were considered in case of proximity of operating point position to linear difference resonance in the presence of nonlinear resonance 2-2. In this case it is possible to make the system integrable by using averaging of fast phases, so this dynamic is regular. In this paper, the theoretical analysis, as well as comparison with an experiment are presented.

1. Introduction

Linear beam dynamic in accelerators is well studied, but in the modern colliders nonlinear effects are gaining importance. The example of such an innovative accelerator is the e^+e^- collider VEPP-2000 [1], which is designed to operate with round colliding beams and its working point is located on the main difference resonance.

It is easy to see from the basic resonance equation

$$l\nu_x + m\nu_y = n,$$

where l, m, n are integer, that such a working point actually stands not only on a single (1-1) resonance ($l = 1, m = -1$), but also on an infinite number of nonlinear coupling resonances, such as (2-2), (3-3) and so on. These resonances result in beam dynamics whose details and consequences are not well understood.

The operating mode of VEPP-2000 can be called “strong coupling”, because two transverse dimensions whose tunes are very close are effectively mixed and form the betatron normal modes. In that situation, any perturbation in the accelerator lattice can excite two-dimensional resonances mentioned above. So it is very important to get insights into that system dynamics.

In this article the contributions of nonlinearities to coupled betatron oscillation are considered with simultaneous action of (1-1) and (2-2) resonances in the VEPP-2000 collider.

Primarily, the general Hamiltonian is derived in the variables of linear eigenvectors, then this Hamiltonian is reduced to one-dimensional difference Hamiltonian and some phase portraits are plotted. Further, the centre-of-charge motion, so as their spectra, of betatron coupled system are investigated and modelled. In the end, predictions are compared with observable spectra, and the main findings are summarized in conclusion.

2. The linear resonance basis

The 4-dimentional Floquet vectors, written in terms of Twiss parameters of coupling-free optics, can be introduced for (1-1) system:

$$Y_A = \begin{bmatrix} \mathrm{e}^{i\left(\chi_x + 2\pi n\frac{n_{\text{рез}}}{2}\right)} w_x \cos\gamma \\ \mathrm{e}^{i\left(\chi_x + 2\pi n\frac{n_{\text{рез}}}{2}\right)} \left(w_x' + \frac{\mathrm{i}}{w_x}\right)\cos\gamma \\ \mathrm{e}^{i\left(\chi_y - 2\pi n\frac{n_{\text{рез}}}{2} - \alpha\right)} w_y \sin\gamma \\ \mathrm{e}^{i\left(\chi_y - 2\pi n\frac{n_{\text{рез}}}{2} - \alpha\right)} \left(w_y' + \frac{\mathrm{i}}{w_y}\right)\sin\gamma \end{bmatrix} e^{2\pi i n(\nu_x + \nu_y + \eta)/2}$$

$$Y_B = \begin{bmatrix} -\mathrm{e}^{i\left(\chi_x + 2\pi n\frac{n_{\text{рез}}}{2} + \alpha\right)} w_x \sin\gamma \\ -\mathrm{e}^{i\left(\chi_x + 2\pi n\frac{n_{\text{рез}}}{2} + \alpha\right)} (w_x' + \frac{\mathrm{i}}{w_x})\sin\gamma \\ \mathrm{e}^{i\left(\chi_y - 2\pi n\frac{n_{\text{рез}}}{2}\right)} w_y \cos\gamma \\ \mathrm{e}^{i\left(\chi_y - 2\pi n\frac{n_{\text{рез}}}{2}\right)} (w_y' + \frac{\mathrm{i}}{w_y})\cos\gamma \end{bmatrix} e^{2\pi i n(\nu_x + \nu_y - \eta)/2}$$

They are called “normal oscillations Floquet vectors”, and the general solution is the linear sum of them (with complex conjugation so that the physical variables are real).

Here $n = s/2\pi\bar{R}$ is dimensionless azimuth, $w_x = \sqrt{\beta_x}, w_y = \sqrt{\beta_y}$, $\eta = \nu_a - \nu_b$ is the difference of mode tunes and coupling angle γ introduced so that $\eta = \sqrt{\delta^2 + |C|^2}, \delta = \eta\cos 2\gamma\,, C = \eta \sin 2\gamma\, e^{i\alpha}$, C is the resonance (1-1)

amplitude, or the coupling coefficient. Basic frequencies obey the equality $\nu_x - \nu_y = n_{res} + \delta$. In numerical simulations the dimensionless azimuth n is treated as integer variable, meaning the revolution number.

3. Nonlinear Hamiltonian

The higher resonance is, the less it's effect, so here we proceed only with (2-2) resonance. It is corresponding to the second order Hamiltonian in action, and to fourth order in coordinates. These terms are generated by:

- quadrupole fringes,
- solenoid fringes,
- colliding beam
- general octupole perturbations.

Below only free betatron oscillations with octupole perturbation are considered, other sources can be treated in the similar way. Name "unperturbed" refers to the system with skew-quadrupole perturbation. In this paper, the impact of mentioned (2-2) sources is considered as perturbation to unperturbed system (1-1), which solution is well-known, then the new eigenvectors are the linear combination of unperturbed ones:

$$\hat{A} = A\, e^{i\,\varphi_a};\ \hat{B} = B\, e^{i\,\varphi_b}$$
$$x = \frac{1}{2}A\, a_1\left(e^{i(\psi_a+\varphi_a)}\right) + \frac{1}{2}B\left(b_1 e^{i(\psi_b+\varphi_b)}\right) + \text{c. c} \qquad (1)$$
$$y = \frac{1}{2}A\left(a_3\, e^{i(\psi_a+\varphi_a)}\right) + \frac{1}{2}B\, b_3\left(e^{i(\psi_b+\varphi_b)}\right) + \text{c. c}$$

Here a_i and b_i are the normal eigenvectors components of unperturbed system, ψ_i are their betatron phases; A, B are the slow amplitudes, φ_a, φ_b are the slow phases, that emerge with perturbation.

Coefficients in this linear decomposition conform with equations [6]:

$$\widehat{\mathrm{A}}' = -i\, Y_A^{*T} SG;\ \widehat{\mathrm{B}}' = -i\, Y_B^{*T} SG \qquad (3)$$

where S is the unit symplectic matrix, G is the vector of perturbations in the equations of motion.

Writing down the obtained equations and switching to the difference variables ($\Phi = 2\pi n\,\eta + \varphi_a - \varphi_b$, $J = J_a - J_b$, $II = J_a + J_b$), the desired Hamiltonian is obtained after integrating over the period and fast phases averaging (see apendix B for details):

$$H = \frac{1}{2}\left((J^2 + II^2)(p+r) + (p-r)(2II\,J)\right) + q(II^2 - J^2) + 4\pi J\eta + 2II\nu_0 + \\ + \sqrt{II^2 - J^2}\left(k_{11}(J + II) + k_{12}(II - J)\right)\cos(\alpha + \Phi) + f_2(II^2 - J^2)\cos(2\Phi) \qquad (4)$$

The equations for the new variables can be obtained from that Hamiltonian:

$$J' = -\frac{dH}{d\Phi}, \Phi' = \frac{dH}{dJ}, \Phi'_{\text{сум}} = \frac{dH}{dII}, II' = 0$$

3.1 System analysis in difference variables

In the difference variables the problem is one-dimensional, which leads to the possibility of 2D-phase space plotting and, therefore, allows one to analyze the system qualitatively. That analysis shows some critical condition, which lower estimation is expressed as $c \equiv \frac{|f_2|\,II}{\eta} = 1$ (so as with substitution $f_2 \to k_{11}, k_{12}$). At this point the phase portrait is altered and several additional fixed points appear.

The linear resonance moves apart the betatron frequencies. So, on the VEPP-2000, η is usually not less than 0,001. This fact, together with the estimates given below, makes it possible to assert that at the values of f_2, k_{11}, k_{12} existing at VEPP-2000, such additional autophasing domains and fixed points are either not formed or their depths are not large. In any case, this resulting in a small redistribution of particles, but non-roundness up to ~20% has almost no effect on the important parameters of the collider, as was found experimentally at the VEPP-2000.

Two different phase portraits are shown in Fig. 1. Additional stationary points are clearly visible.

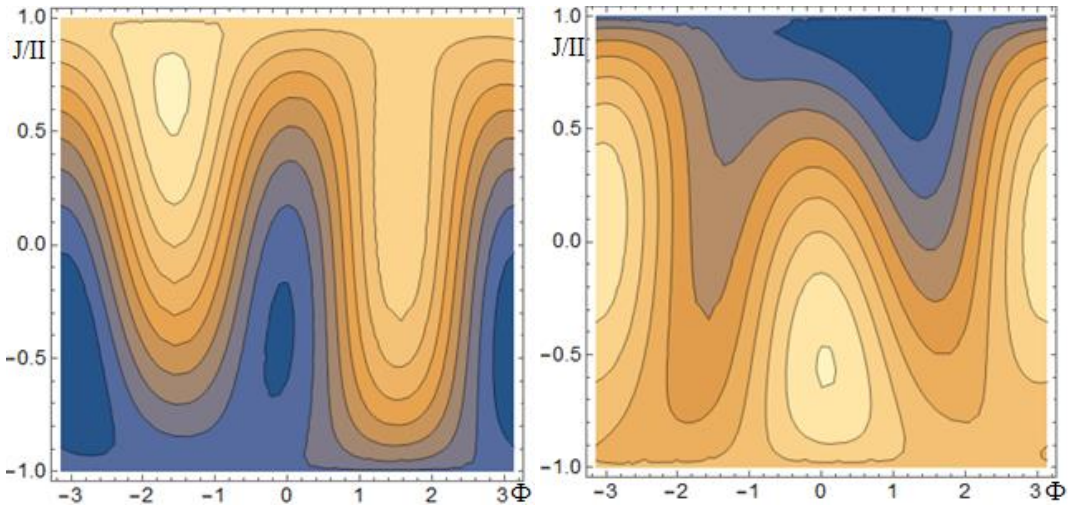

Fig. 1. Phase portraits with strong nonlinearities (with additional autophasing areas)

Stability is determined by the matrix of the quadratic form of the Hamiltonian, linearized near stationary points:

$$A = \left(\begin{matrix} \frac{\partial^2 H}{\partial J^2} & \frac{\partial^2 H}{\partial J \partial \phi} \\ \frac{\partial^2 H}{\partial J \partial \phi} & \frac{\partial^2 H}{\partial \phi^2} \end{matrix} \right) \Bigg|_{(\phi_0, J_0)}$$

In the Hamiltonian system, the possible types of stationary points are saddle and center. Their stability is determined by the sign-definiteness of the quadratic form: a point is stable (center) if $detA > 0$ and unstable (saddle) if $detA < 0$.

Typical cases of $J_{stationary}(n)$ dependence are shown in fig. 2.

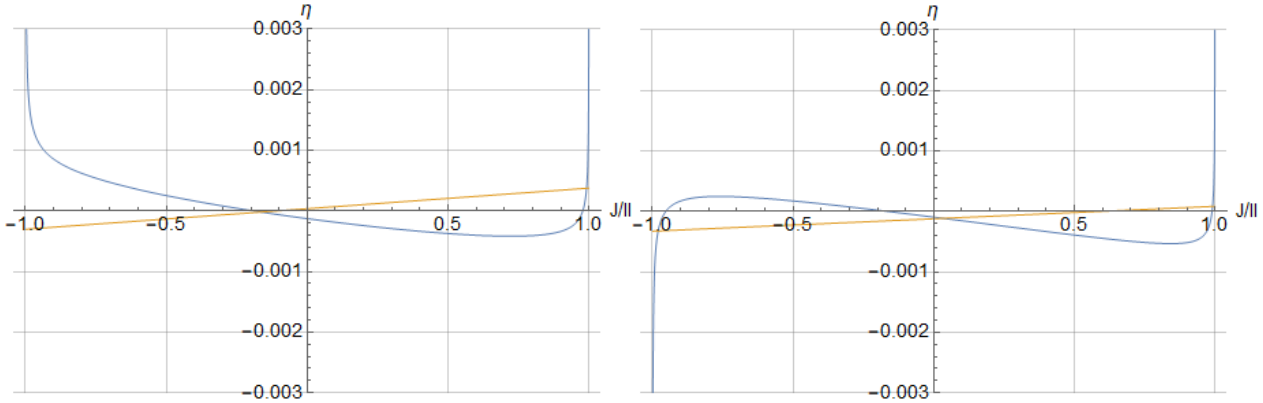

Fig 2. $\eta(J_{stationary})$ dependence examples

In total, for a given η, the existence of 0 to 4 fixed points is possible, with no more than 3 centers and no more than 1 saddle.

Due to the preservation of the sum action, it is convenient to plot phase trajectories on a II radius sphere. In these portraits the I/II ratio is plotted along the z-axis, and the polar angle represents the difference phase Φ. Several typical cases of such portraits are shown in fig. 3: the symmetric cases with 2 (a) and 3 (b) stationary points, and general non-symmetric case with saddle point (c). Each Fig. 3 row represents one phase portrait, drown from different points of view. The shift α is equal to 0 in each portrait for the ease of observation.

Also the phase portraits without (a), with slight (b), and with large (c) nonlinearities are presented in Fig. 4 in order to show the complications caused by resonances.

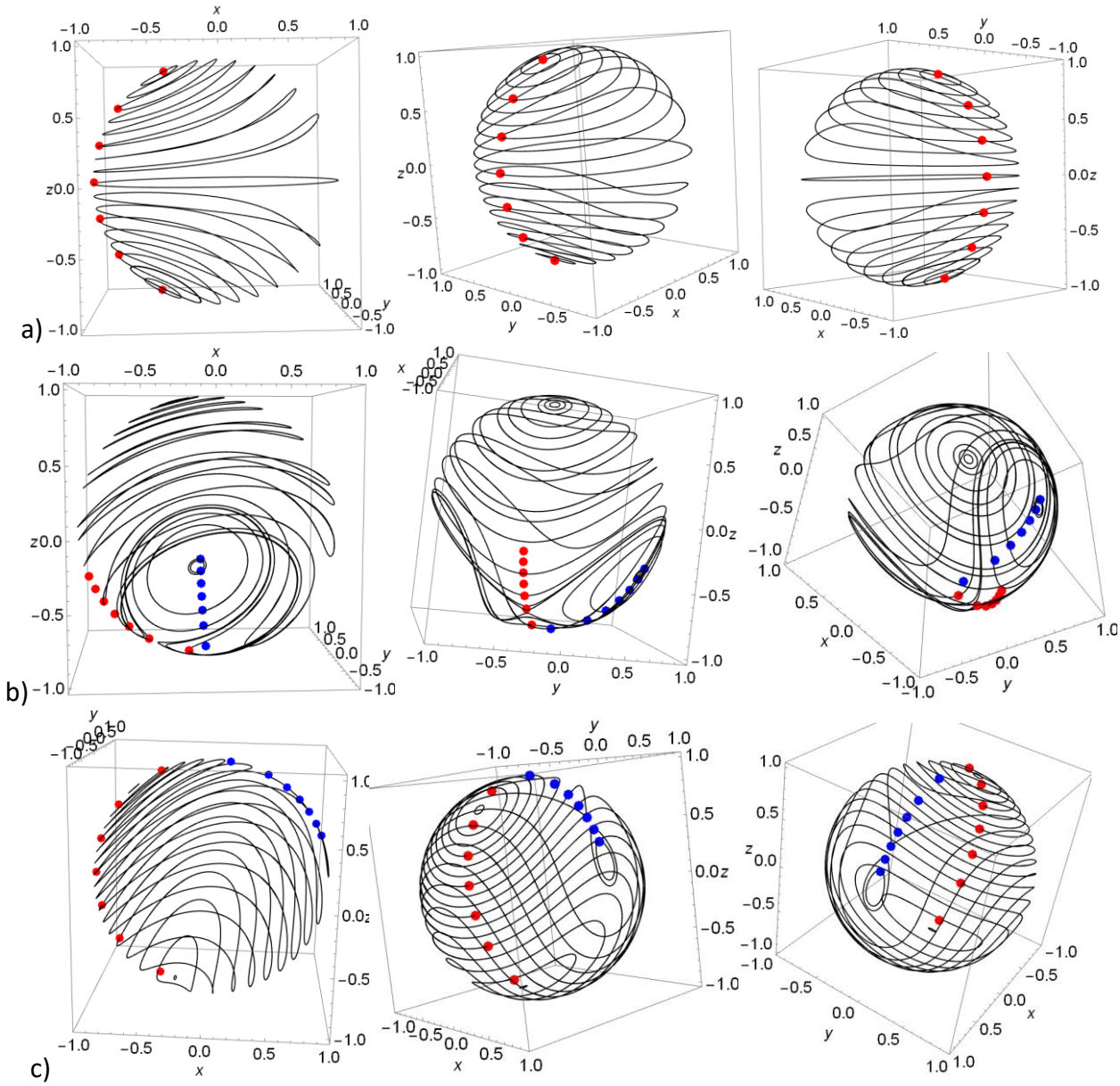

Fig. 3. Phase portraits of free betatron oscillations in 1-1+2-2 system

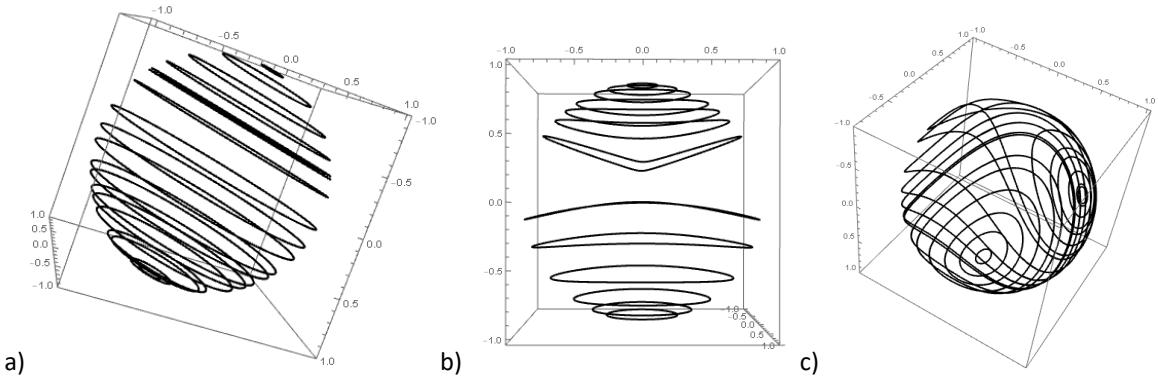

Fig 4. Phase portraits without (a) and with different (b, c) nonlinearities

4. Signal modeling

The presence of the nonlinearities described above is indicated by the decoherence in the signals from BPMs – the beam dipole moment disappears after ~ 1000 revolutions. The decoherence theory is well described in [3, 4] for uncoupled oscillations, and it is applicable to mode signals.

Assuming that nonlinearities strength is small ($c = \frac{|f_2|\ II}{\eta} \ll 1$), we obtain expressions for phases φ_a and φ_b in the first order of smallness for Hamiltonian (3) (P 1):

$\varphi_a(n) = (q\ b_2^2 + p\ b_1^2)\ n,\ \ \varphi_b(n) = (q\ b_1^2 + r\ b_2^2)\ n$

Where $b_1 = \sqrt{2J_a}, b_2 = \sqrt{2J_b}$ are the average oscillation amplitudes. Resonances appear only in the second order, so in the current situation $A, B = const$.

The comparison with BPM data reveals that the constant-nonlinearity coefficients are not small, $p, q, r \sim \eta/II$ in order of magnitude. Assuming that all nonlinear coefficients in Hamiltonian are of the same order, we can conclude, that coefficient c is also not small in general case, and the system is approximately on the verge of additional fixed points emergence. One of the modeled BPM signals is shown in Fig 6.

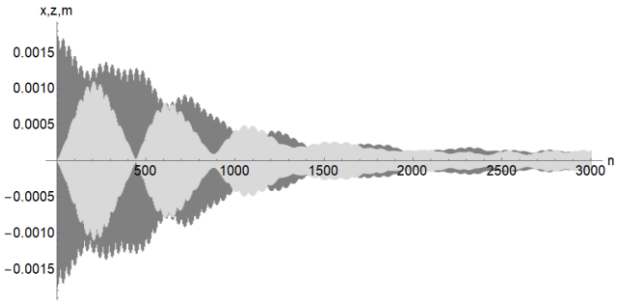

Figure 6: Betatron history modeling example.

4.1 Solo particle oscillation spectra

In the presence of $2-2$ resonance, the actions, obviously, cease to be constants, and oscillate at the double frequency 2η as well as phases. The amplitude of these oscillations and frequencies shifts are proportional to c^2. The same effect is produced by $1-1$ resonance, exciting oscillations with a single η. When passing to the observable x-y coordinates, the spectra of the modes are added with the weights that are the components of the vectors of normal oscillations in accordance with the linear expansion of the coordinates into modes.

For different parameters, the mode frequencies are shifted, increasing or decreasing the distance between the main peaks, denoted below as η_1. As a result, in the Fourier analysis of the dipole moment oscillations, two shifted fundamental frequencies ν_x and ν_y are visible, and one or more equidistant satellites responsible for phase oscillations in the autophasing domains on single and double η_1.

The series of signal modeling were made for collective (see Fig. 3), as well as for single particle dynamics. Simulations were made based on numerical solutions of averaged Hamiltonian (3) equations. Further only single particle simulations are considered due to their superior accuracy. Also, all the spectra below belong to the mode motion, namely, mode A. The spectrum of mode B, obviously, does not contain significant differences and the transition to x-y is carried out as described above.

Some results are shown in Fig. 7. Blue and red lines mean B and A mode tunes respectively. The spectra correspond to different initial parameters on the first phase portrait from the Fig. 3, showed by dots:

Fig. 7a) ↔ Fig. 3a) red dots, in order of J increasing.

Fig. 7b) ↔ Fig. 3b) red dots, in order of J increasing.

Fig. 7c) ↔ Fig. 3c) blue dots, in order of J decreasing.

As was expected, the obtained Fourier spectra show several peaks, the distance η_1 between them depends on the proximity of the trajectory to the separatrix – it is inverse to the period of revolution around the fixed point. For trajectories located far from fixed points and separatrices, the spectrum shows the main mode oscillations and small satellites. At fixed points, the actions and the difference phases are constant, and only the line with the frequency of the given mode is visible. When a particle trajectory passes close to the saddle point, the frequency of the phase oscillations decreases, and the spectrum shows many lines that are close to each other.

In Fig. 8 the mode oscillations near a separatrix (1st graph), and near a fixed point (2nd graph) are shown. It can be seen from them that, indeed, near the separatrix, many harmonics are observed. The periodicity of the envelope clearly indicates that the spectrum of such oscillations is linear.

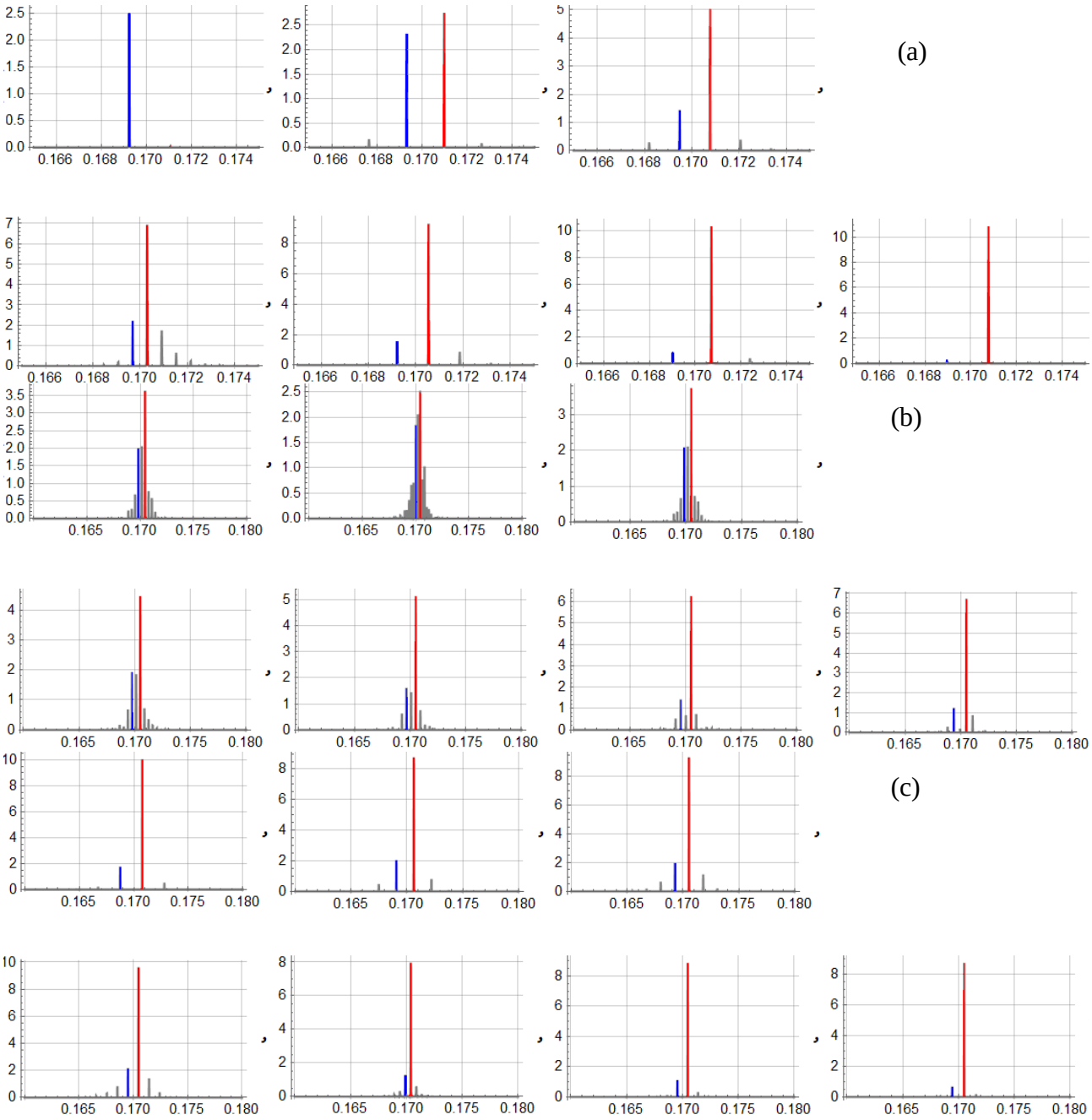

Fig. 7. Fourier spectra in terms of a-b modes with close to each other k_{11} and k_{12}

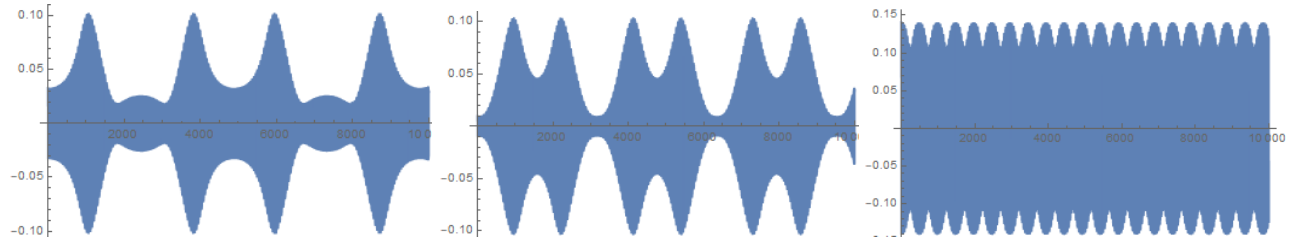

Fig. 8. Particle mode oscillations near separatrix

5. VEPP-2000 nonlinearities estimation

As mentioned above, three main sources of third order nonlinearities, producing $2-2$ resonance, are the solenoid, quadrupole fringes and colliding beam action. We will treat them consistently. The exact calculation of the coefficients is rather difficult and complicated by the lack of accurate quantitative measurements of the fields at the edges of solenoids and quadrupole lenses. Especially the latter, due to their complex inclusion in achromatic blocks. Nevertheless, it is possible to estimate order of magnitude taking as basis the model of "Maxwellian" edge fields.

5.1 Solenoid fringes

Undeniably important elements of VEPP-2000 collider are the final focusing solenoids. They have nonlinear, beam rotating radial field on the fringes and therefore contribute to tunes amplitude dependence.

$$B_x = H'(z)x + \frac{H'''(z)}{16}(x^3 + y^2x)$$
$$B_y = H'(z)y + \frac{H'''(z)}{16}(x^2y + y^3)$$

The x equation includes B_y and vice versa. It is seen that these sources contribute even powers of x and y (for example, x^4 or x^2y^2) to the Hamiltonian. The coefficients in the Hamiltonian are multiplied by the square of the actions, and are obtained by integrating the fields with squares of the beta functions weights.

Actions are easy to estimate – from geometric parameters of lattice, beta functions and amplitudes of betatron oscillations, so J is in order of 10^{-4}. Resonance strength was already estimated without circular modes in [4]: $f_2 \sim 100$ см$^{-1}$. When estimating in a simple way - substitution of fields in the form of perturbations (see Appendix), f_2 is roughly represented as $Lh_3\beta^2$, where $h_3 = \frac{H'''(s)}{16B\rho} \sim 10^{-2}$, resulting in the same value. So we have $c \lesssim 10$, which, as turns out, does not differ much from the critical case of the qualitative complication of phase portraits and the appearance of additional regions of betatron autophasing.

5.2 Quadrupole fringes

To estimate the contribution of quadrupole lenses to cubic nonlinearity, we will assume that the contributions from each edge can be summed up, neglecting the influence of other closely spaced collider elements.

Fields created at the edges of the quadrupole lenses (see appendix):

$$H_x = G(z)y - \frac{G''(z)}{12}(3x^2y + y^3)$$
$$H_y = G(z)x - \frac{G''(z)}{12}(x^3 + 3xy^2)$$
$$H_z = G'(z)xy$$

For simplicity, we will assume that the length of the edge fields is small, and the quadrupole gradient G undergoes a jump from 0 to G_0 at the lens boundary.

Using the same perturbation method, we substitute the written fields as a perturbation of the equations of motion due to the Lorentz force:

$$G_x = \frac{1}{B\rho}(y'H_z - H_y), G_y = -\frac{1}{B\rho}(x'H_z - H_x)$$

For simplicity of estimation, assume that the system is not coupled, and the eigenvectors are ordinary one-dimensional Floquet vectors. Doing the same as in octupole Hamiltonian calculating, we first integrate the perturbation with weight in accordance with formula (2) (we average over the betatron phases $\psi x, \psi y$), and then we integrate over z (s or t) – over the section with the boundary field - here it is a small region near the gradient jump. Here, due to the presence of the second derivative of the gradient, which is the first derivative of the delta function, it is necessary to integrate by parts. Finally, amplitude-dependent frequency shifts can be introduced:

$$\begin{aligned}\Delta\varphi_x &= \frac{G_0}{4B\rho}\left(w_x^3w_x'J_x + \left(w_y^2w_xw_x' - w_x^2w_yw_y'\right)J_y\right)\\ \Delta\varphi_y &= \frac{G_0}{4B\rho}\left(\left(w_y^2w_xw_x' - w_x^2w_yw_y'\right)J_x - w_y^3w_y'J_y\right)\end{aligned} \quad (6)$$

The same result can be reached through the Hamiltonian approach; such a study was done in the work [11].

Now we need to summarize this result over whole accelerator circumference. As was mentioned, we will assume all lenses thin with strength $\frac{1}{P}, P = \frac{G_0L}{B\rho}$. In that case beta functions at entrance and exit are match, and $\Delta w' = -Pw$. Summarizing (6) over one lens (with keeping in mind that $G'_{entrance} = -G'_{exit}$):

$$\begin{aligned}\Delta\varphi_x &= \frac{G_0P}{4B\rho}\left(w_x^4J_x + 2w_y^2w_x^2J_y\right) = \left(\frac{G_0}{B\rho}\right)^2\frac{L}{4}w_x^2\left(w_x^2J_x + 2w_y^2J_y\right)\\ \Delta\varphi_y &= \left(\frac{G_0}{B\rho}\right)^2\frac{L}{4}w_y^2\left(2w_x^2J_x + w_y^2J_y\right)\end{aligned} \quad (7)$$

After summarizing over all VEPP-2000 lenses, data of which is introduced in table 1 [9], the nonlinearities (p, q, r) estimation is obtained:

$$p \sim 2.5; q \sim 1.5; r \sim 1.6,$$

Which is noticeably less than from solenoids.

The formula for the edge nonlinearities in terms of normal modes $a - b$ (using basis (1)) is not presented here due to its cumbersomeness.

Table 1. Basic parameters of quadrupole lenses of one quadrant of the VEPP-2000 magnetic structure. The fields are given for a ring energy 1 GeV.

Линза	Длина, см	Градиент, кГс/см	Бета-x, м	Бета-z, м
F1	6	0.995	7.5	7.5
D1	14	-1.16	3	3.5
F2	19	4.7	6	2.7
D2	14	-2.53	4	4
D3	14	-4.77	0.5	4
F3	14	4.94	1.5	1.5

5.3 Colliding beam

The radial force, produced by colliding Gaussian beam is well-known. It is shown schematically in fig. 9. Here n is linear particle density in the beam:

$$F_r(r) = -2n\,e^2\,(1+\beta^2)\frac{1}{r}\left(1-\exp\left(-\frac{r^2}{2\sigma^2}\right)\right) \quad (8)$$

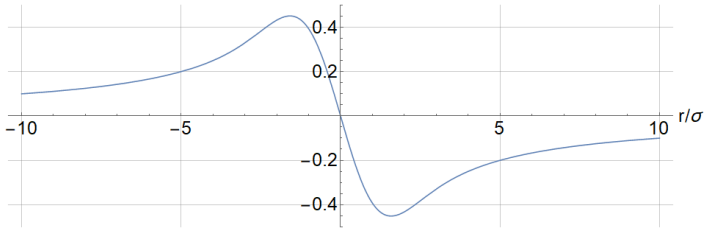

Fig. 9. Amplitude dependence of the radial force caused by the colliding beam

After the integrating of (8) over the entire collision area, assuming normal longitudinal distribution, we arrive to angular displacement obtained by particle during the collision:

$$\Delta r' = -f\frac{\sigma^2}{r}\left(1-\exp\left(-\frac{r^2}{2\sigma^2}\right)\right), f = \frac{4Nr_e}{\gamma\sigma^2} \quad (9)$$

For a particle arriving almost "head-on" (with small amplitudes) to the colliding beam, this force is linear in amplitude and acts like a quadrupole lens with force f, except that it focuses (defocuses) in both directions. Such a lens creates a constant frequency shift approximately equal to the interaction coefficient of colliding beams ξ. For larger amplitudes, the force becomes nonlinear and, in particular, generates cubic nonlinearity.

In order to obtain rough estimation of nonlinearities, expand the resulting expression to the second order, and, using the tune shift Hamiltonian $H = J\xi$, and substituting $r \to \sqrt{J}\beta^*$, the estimation of f_2 produced by colliding beam is obtained:

$$f_2 \sim \frac{\xi\beta^{*2}}{\sigma^2} \sim 10^5$$

This turns out to be a huge value, and, indeed, at VEPP-2000 β^*, beta function at the meeting point, is about 10 cm, which leads to amplitudes of ~ 0.1 cm, which is about 10 times greater than σ, and, therefore, the exponential expansion cannot be used. The record VEPP-2000 $\xi \sim 0.1$ also makes a large contribution to the nonlinearity. In reality, the effect of the of the colliding beam nonlinearity is not so huge – this can be seen, for example, from Fig. 9 – the force is small at large amplitudes.

6. experimental observations

Predicted spectrum patterns were prepared to compare with the experimental observables. Presently but a little time was available for this experiment.

The measured spectra (two of them are shown in Fig. 6) are not rich for satellites, and comparing with the series of predicted spectra, it can be concluded, that the resonance terms are weaker or slightly above the critical values, as was estimated from the decoherence time, and conclusions from the measurements are preliminary.

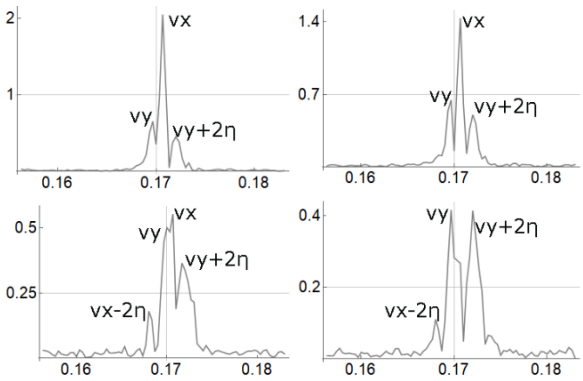

Figure 6: x (top), and y (bottom) spectra, observed after kicks on the VEPP-2000.

Sure, more experimental data is needed to prove the resonance $2-2$ influence on the particle motion on the VEPP-2000 collider.

7. Conclusion

A system with several closely spaced resonances can be reduced to integrable form using fast-phase averaging, so that its dynamics is regular.

The simultaneous action of resonances 1-1 and 2-2 was considered. The phase portraits were plotted and analyzed, the qualitative features, auto-phasing domains and fixed points were found.

Strengths of VEPP-2000 cubic nonlinearities resulting in the resonance term amplitude were estimated. The comparison with decoherence time showed the qualitative agreement of estimations and measurements.

Extensive series of modeling the betatron motion were performed with different phase-space patterns. Fourier spectra of those oscillations were predicted in both normal-mode and observable coordinates.

Series of spectra from the routine operating mode of the collider were compared with predicted ones. The comparison showed a fairly good agreement, but a dedicated validation experiment is required to get more data.

References

1. V. N. Litvinenko, E. A. Perevedentsev. Beam parameters calculation in accelerators with coupling. VI USSR charged particle accelerator meeting, v. II. 1979.
2. R. D. Ruth. Single particle dynamics and nonlinear resonances in circular accelerators. SLAC-PUB-3836. 1985.
3. V. V. Danilov, E. A. Perevedentsev, et al. Dynamic aperture limitation in storage ring due to solenoids. Institute of Nuclear Physics, Novosibirsk. EPAC1990.
4. W. Herr, T. Pieloni. Beam-Beam Effects. CERN Yellow Reports: School Proceedings, Vol. 3/2017, CERN-2017-006-SP.
5. E. A. Perevedentsev. Linear beam dynamics and beyond. High quality beams. New York. 2001.
6. S. Y. Lee. Decoherence of the kicked beams II. Indiana University. SSCl-N-749. 1991.
7. M. G. Minty, A. W. Chao, W. L. Spence. Emittance growth due to decoherence and wakefields. Particle Accelerator Conference, 1995, vol.5.
8. D. B. Shwartz. Round beams in VEPP-2000 collider: PHD. BINP. 2013.
9. E. Forest. Leading order hard edge fringe fields effects exact in $(1+\delta)$ and consistent with Maxwell's equations for rectilinear magnets. Nuclear Instruments and Methods in Physics Research A269 (1988) 474-482.

Appendices

a) Octupole nonlinearities Hamiltonian

The general shape of octupole fields:

$$H_x = h_3(3x^2y - y^3)$$
$$H_y = h_3(x^3 - 3xy^2)$$

From here the G components are obtained:

$$G_4 = H_x, G_2 = -H_y.$$

Substituting G to (2), the sum of modes is obtained:

$$A' + i\,A\,\varphi_a' = \sum_{k,l=-4}^{4} c_{kl} e^{i(k\,(\varphi_a+\psi a)+l\,(\varphi_b+\psi b))}$$

The exponent extents are presented as:

$$i\left(k\,\varphi_a + l\,\varphi_b + \left(\nu + n_q\right)\frac{s}{R}\right),$$

where $\nu + n_q$ – some resulting frequency, ν and n_q – its fractional and integer parts, respectively, s – longitudinal coordinate, $\bar{R}$ – mean radius of the particle orbit. Further, it is necessary to average the obtained equations over the period of particles revolution in the collider. The terms on the right-hand side, for which the frequency ν in the exponent is not small (the resonance condition is not fulfilled), are averaged to 0. The exponents with slow phases can be taken out from the averaging integral, and, as a result, the averaged equations have the form:

$$A'(n) + i\,A(n)\varphi_a'(n) = 2\pi\bar{R}\sum_{k,l=-4}^{4}\overline{c_{kl}}e^{i(k\,\varphi_a + l\,\varphi_b + \nu 2\pi n)}$$

$$\overline{c_{kl}} = \frac{1}{2\pi\bar{R}}\oint_0^{2\pi\bar{R}} c_{kl}e^{i(n_q\frac{s}{\bar{R}})}\,ds$$

and similarly for B. Here $n = s/2\pi\bar{R}$ is the turnover number. The sum of the coefficients is complex and must be calculated separately for each source of nonlinearities with different fields. We introduce here the coefficient for the main resonance of this work:

$$\begin{aligned}\overline{c_{2-2}} = -\frac{3i}{64}AB^2\oint_0^1 h_3 e^{-2i(\chi_x+\chi_y+2\pi n\,n_{\text{рез}})}\big[-\beta_x^2 e^{2i(\alpha+\chi_x+\chi_y+2\pi n\,n_{\text{рез}})} + \\ +\big(3e^{4i(\alpha+\chi_x+2\pi n\,n_{\text{рез}})} - 4e^{2i(\alpha+\chi_x+\chi_y+2\pi n\,n_{\text{рез}})} + 3e^{4i\chi_y}\big)\beta_x\beta_y - \\ -e^{2i(\alpha+\chi_x+\chi_y+2\pi n\,n_{\text{рез}})}\beta_y^2 - 4\big(e^{4i(\alpha+\chi_x+2\pi n\,n_{\text{рез}})} - e^{4i\chi_y}\big)\beta_x\beta_y\cos(2\gamma) + \\ \big(e^{4i(\alpha+\chi_x+2\pi n\,n_{\text{рез}})}\beta_x\beta_y + e^{4i\chi_y}\beta_x\beta_y\big)\cos(4\gamma) + \\ +e^{2i(\alpha+\chi_x+\chi_y+2\pi n\,n_{\text{рез}})}\big(\beta_x^2 + 4\beta_x\beta_y + \beta_y^2\big)\cos(4\gamma)\big]\,dn\end{aligned}$$

Initially, in the general case, the coefficients $\overline{c_{kl}}$ are complex. For convenience we add their phases to the exponents, then all the coefficients in the equations are real. In this problem, the proximity of the average frequency to either 1/2 or 1/4 was not assumed, therefore, upon averaging over a large period of time, only terms with slowly oscillating exponents remain - the sought resonances $2-2$ and $1-1$, as well as the constant mode:

$$\begin{aligned}A' + i\,A\,\varphi_a' = ipA^3 + i\left(\frac{3}{2}A^2B\,k_{11} + \frac{1}{2}B^3\,k_{12}\right)e^{-i\,(\varphi_a-\varphi_b+2\pi n\,\eta+\alpha)} + \\ +if_2\,A\,B^2\left(\frac{q}{f_2} + e^{-i\,(2\varphi_a-2\varphi_b+4\pi n\,\eta)}\right) \\ B' + i\,B\,\varphi_b' = irB^3 + i\left(\frac{1}{2}A^3\,k_{11} + \frac{3}{2}AB^2\,k_{12}\right)e^{-i\,(\varphi_a-\varphi_b+2\pi n\,\eta+\alpha)} + \\ +if_2B\,A^2\left(\frac{q}{f_2} + e^{-i\,(2\varphi_a-2\varphi_b+4\pi n\,\eta)}\right) \\ H = 2\left(k_{11}J_a^{\frac{3}{2}}\sqrt{J_b} + k_{12}J_b^{\frac{3}{2}}\sqrt{J_a}\right)\cos(\varphi_a - \varphi_b + 2\pi n\,\eta + \alpha) + \\ +(pJ_a^2 + rJ_b^2 + 2qJ_aJ_b) + 2f_2J_aJ_b\cos(2\varphi_a - 2\varphi_b + 4\pi n\,\eta)\end{aligned} \qquad \text{(A.1)}$$

Where $\eta = \nu_{a0} - \nu_{b0}$ – initial mode frequencies spacing, $J_a = \frac{A^2}{2}$, $J_b = \frac{B^2}{2}$, and the initial phases were redesignated so that only resonance $1-1$ has a constant displacement α (here it is not the same as in the eigenvectors of mode oscillations (1)). It should be noted right away that all the coefficients in the general case are of the same order, since all are proportional to h_3, the strength of the perturbation. The rest of the sources of cubic nonlinearity give a Hamiltonian of the same form, with a difference only in the coefficients. We will consider the general case of all coefficients that are not equal to zero, and here we only mention that the introduced p and r for the edges of the solenoid are equal to zero.

To obtain the complete Hamiltonian of the system, the unperturbed averaged Hamiltonian should also be added to it: $H_0 = (J_a + J_b)2\pi\nu_0 + (J_a - J_b)2\pi\eta, \nu_0 = \frac{\nu_{a0}+\nu_{b0}}{2}$. One can observe, that $J_a' = -J_b'$, whence it follows that the total action is preserved: $II = J_a + J_b$. The appearance of an additional integral of motion means the fulfillment of Liouville's theorem about integrable systems and makes it possible to reduce the problem to a one-dimensional one.

Introducing of the difference J and the sum II action allow to get rid of one variable. Lowering further the dimension of the problem, we denote the difference phase in parentheses $\Phi = 2\pi n\,\eta + \varphi_a - \varphi_b$. Accurately writing down the Hamiltonian equations (or using the generating function), we arrive to a new Hamiltonian:

$$\begin{aligned}H = \frac{1}{2}\big(p(J^2 + II^2 + 2II\,J) + r(J^2 + II^2 - 2II\,J)\big) + q(II^2 - J^2) + 4\pi J\eta + 2II\nu_0 \\ +\sqrt{II^2 - J^2}\big(k_{11}(J + II) + k_{12}(II - J)\big)\cos(\alpha + \Phi) + f_2(II^2 - J^2)\cos(2\Phi)\end{aligned}$$

Whence new variables equations are obtained:

$$J' = -\frac{dH}{d\Phi}, \Phi' = \frac{dH}{dJ}, \Phi'_{\text{сум}} = \frac{dH}{dII}, II' = 0$$

b) Solenoids and quadrupole lenses fringe fields. Cubic nonlinearity

Consider the edge of a quadrupole lens. Let it have a finite length, the field inside is constant along the axis and has a gradient G, and sharply decreases at the ends. The standard introduced scalar potential Ψ ($B = -\nabla\Psi$) must satisfy the Laplace equation. In the main part of the quadrupole, it will then have the form $-\Psi = G\,xy$. In view of the axial symmetry, it is convenient to solve the problem at the edges in cylindrical coordinates. In this part, the derivatives of the gradient are nonzero and should be taken into consideration. Assuming that the main term

$\frac{1}{2}G(z)\,r^2\,sin(2\varphi)$ remains the main term, we obtain the Laplacian: $\frac{1}{2}G''(z)\,r^2\,sin(2\varphi) = 0$, whence we conclude that in the potential must also include a term with the second derivative of the gradient. Continuing iterations, we find the first terms of the expansion:

$$-\Psi = G(z)xy - \frac{G''(z)}{12}(x^2+y^2)xy + \cdots$$

$$B_x = G(z)y - \frac{G''(z)}{12}(3x^2y + y^3)$$

$$B_y = G(z)x - \frac{G''(z)}{12}(x^3 + 3y^2x)$$

The solenoid contribution is calculated in a similar way. One can also immediately see the answer in [10]:

$$B_x = H'(z)x + \frac{H'''(z)}{16}(x^3 + y^2x)$$

$$B_y = H'(z)y + \frac{H'''(z)}{16}(x^2y + y^3)$$